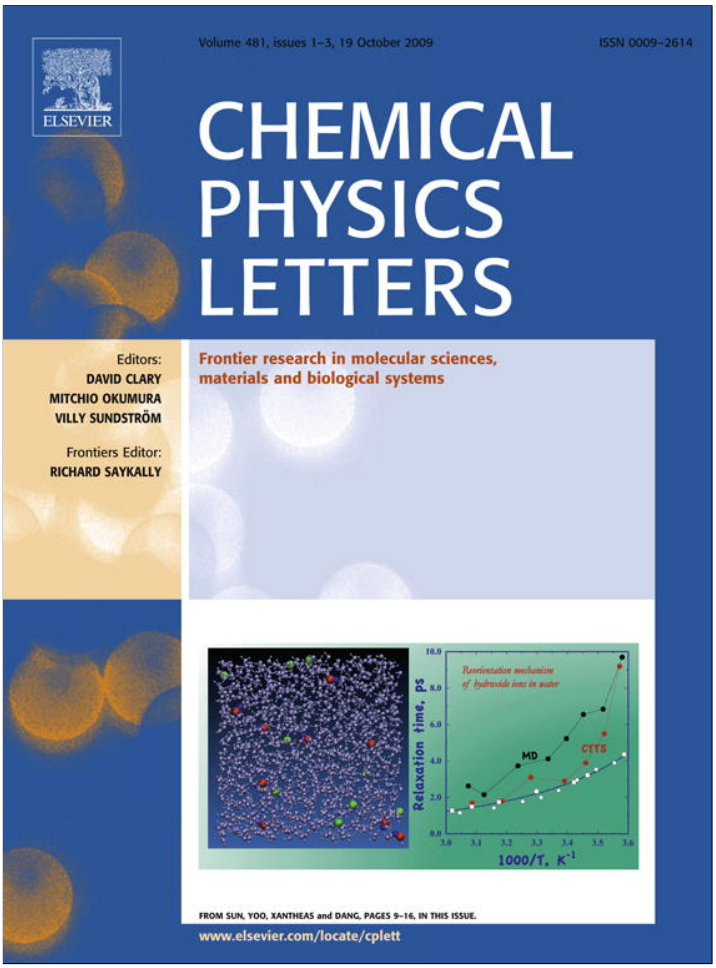

Chemical Physics Letters 481 (2009) 124–129

Contents lists available at ScienceDirect

Chemical Physics Letters

journal homepage: www.elsevier.com/locate/cplett

Atomistic simulations of spontaneous formation and structural properties of linoleic acid micelles in water

Stéphane Abel [a,*], Judith Attia [b], Samy Rémita [d,b], Massimo Marchi [a], Wladimir Urbach [c,e], Michel Goldmann [b,c]

[a] Commissariat à l'Energie Atomique, DSV/iBiTEC-S/SB2SM, Service de bioénergétique, biologie structurale et mécanismes, Gif-sur-Yvette F-91191, France
[b] Institut des Nanosciences de Paris, CNRS UMR7688 – UPMC Paris VI, 140 rue de Lourmel, 75015 Paris, France
[c] Université Paris Descartes, 45 rue des Saint Pères, 75006 Paris, France
[d] Conservatoire National des Arts et Métiers, Chaire de génie analytique, EA4131, 292 rue Saint-Martin, 75141 Paris Cedex 03, France
[e] Laboratoire de Physique Statistique de l'Ecole Normale Supérieure de Paris CNRS UMR8550 – UPMC Paris, Université Paris Diderot, Paris, France

ARTICLE INFO

Article history:
Received 5 June 2009
In final form 13 September 2009
Available online 16 September 2009

ABSTRACT

Molecular dynamics simulations were used to explore the structure of linoleic acid (LIN) micelles with 60 monomers in explicit water. To examine micellar properties, two approaches were considered using 'preformed' and 'self-aggregated' micelles. Our results demonstrate the quickness of the process of monomers aggregation. After 10 ns, both 'preformed' and 'self-aggregated' micelles are characterized by very similar structural properties: a slightly ellipsoidal shape and dimensions close to 20 Å. In addition, 'preformed' and 'self-aggregated' micelles display mainly hydrophobic surfaces, since these latter are made up of ~73% of LIN tails. Finally, within the two kinds of micelles, LIN molecules are bent due to their *cis* double bond conformations.

1. Introduction

Linoleic acid (LIN) is an unsaturated fatty acid (C18:2 (n-6)) containing 18 carbon atoms, two *cis* double bonds, the first being located at the sixth carbon from the end (ω-6 fatty acid), and a polar carboxylic acid headgroup. It is found as a lipid residue into cell membranes [1]. It is also abundant in many vegetable oils (such as sunflower oil). In addition, LIN is widely used in food or cosmetic industries [2] and can serve as template for production of metal nanoparticles (see for example Ref. [3]).

At ambient temperature, fatty acid molecules are not soluble in water in their protonated form. On the contrary, in alkaline media, deprotonated linoleate molecules are known to form various structures depending on the effective pH, the ionic strength and lipid concentration [4–6]. Such as other C18 deprotonated fatty acids, sodium linoleate presents, above pH 9–10 [7,8], an isotropic phase and aggregates into micelles above its critical micelle concentration which was estimated around 2 mM at pH 11.4 [9]. In particular, studies on sodium oleate (C18:1) showed that this phase exists up to a concentration approaching 20% in weight [10,11]. Structures concerning LIN microemulsions were poorly studied and data about linoleic acid systems are very rare in the literature. Twenty years ago, Johnson et al. studied at 40 °C by Small Angle Neutrons Scattering (SANS) potassium linoleate structures near 0.1 M [12]. More recently, Attia et al. used Transmission Electronic Cryo-Microscopy (Cryo-TEM) to examine the structure of sodium linoleate micelles in the presence of silver ions in aqueous solutions at pH 11.5 [3].

In the last decades, molecular dynamics simulation (MD) methods offered powerful tools to study various surfactant structures in different mesophases [13]. Now, they are routinely used to examine micelles at the atomic level to gather information on the fine micellar structures when experimental methods fail. Generally, in MD studies, the aggregates are constructed 'preformed' to save time and computational resources. With the enhanced computer performances, it is now possible to examine the aggregation kinetics [14–17] and the influence of the protocol (i.e. 'preformed' vs. 'self-aggregated') on the micellar structure. The aggregates obtained by the two approaches are most often similar but they sometimes differ significantly.

To examine this aspect and gather more structural data on LIN micelles in water, we present, in this Letter, molecular simulation of the structure of a micelle made up of LIN monomers solvated in explicit water at ambient condition. We examined the influence of the protocol (preformed vs. self-aggregated) used to construct LIN micelles, on the micellar structure. As indicated above, sodium LIN molecules were experimentally shown to form micelles at high pH. However, since classical MD cannot be performed at this pH value, the simulations described in this Letter were performed only at neutral pH, with Na^+ cations as counterions. This difference in pH should have a minimal effect since all molecules in the system were inserted in their deprotonated form as they would be found at basic pH. At high ionic strength, it is admitted that the major

* Corresponding author.
E-mail address: stephane.abel@cea.fr (S. Abel).

0009-2614/$ - see front matter © 2009 Elsevier B.V. All rights reserved.
doi:10.1016/j.cplett.2009.09.033

impact on the ionic layer around the micelle is due to the counterions rather than to the HO^- ions [18]. In addition, sodium cations and linoleate (carboxylate groups) are supposed to form ion pairs due to the dominant short range ion–ion effects [19].

2. Model constructions and simulation methods

Micelles are usually defined with spherical or spheroidal core–shell models consisting of a liquid core of hydrocarbon chains and of a shell gathering polar headgroups with counterions and/or water molecules. Allying a small surface per polar head and a highly curved chain, LIN molecule does not fit in the classical description of single-tail surfactant molecules. In addition, the double bonds, slightly polar and already involved in the increased solubility of the poly-unsaturated linoleic acid compared to the saturated stearic acid [10], are expected to migrate towards the surface. These considerations lead us to an only partially hydrophilic micelle surface. Thus, we suggest a simple model that accounts for micelles exhibiting a significant amount of methyl groups at its surface, emphasized by the parameter *f*, fraction of polar surface over the total micelle surface.

2.1. Geometric description of the linoleic micelle

The deprotonated linoleic acid molecule displays a carboxylate headgroup, that occupies a surface (S_h) close to the section of the CH_2- groups (21 Å^2) in the alkyl chain of the lipid, as observed in 2D Langmuir films [20]. Thus, one can assume that the volume of the molecule is equivalent to that of a cylinder of appropriate dimensions. In addition, if all the headgroups are at the micellar surface and assuming that the micellar hydrophobic core contains only parts of the alkyl chains, the following relations describe the volume (V_m) and surface (S_m) of the spherical micelle:

$$V_m = NLS_h = \frac{4}{3}\pi R_M^3 \qquad S_m = (1+x)NS_h = 4\pi R_M^2 \tag{1}$$

where x is the number of CH_2 groups of each molecule located at the micelle surface ($0 < x \leqslant 17$), N is the aggregation number, and R_M the micelle radius, respectively. Combining the two expressions, we obtain $3L = (1 + x)R_M$. To estimate the stretched lipid length, L, we used Johnson's model of the hydrophobic double bonded chain (21.8 Å – different from Tanford's value 23 Å for saturated 17-carbon chain [21]), and added the size of the headgroup (sphere of radius 1.82 Å). In this description, the polar fraction f values $1/(1 + x)$. For aggregation numbers N varying from 45 to 90 molecules, the R_M and the polar fraction values obtained vary from 17.0 Å to 21.4 Å and from 23.8% to 30.0%, respectively. We compared these values with those obtained from four MD simulations performed with 'preformed' LIN micelles with N values of 45, 60, 75, and 90 at the same lipid concentration and thermodynamic conditions (results not shown). We found that R_M and f are respectively between 8.0% and 16.4%, and between 4.0% and 58.8% larger than the geometrical model predictions. Nevertheless, the best agreement is obtained for $N = 60$ with $R_M = 19.5$ Å and $f = 26.4\%$ where the differences between the model and the simulation values are close to 8.4% and 4.5% for R_M and f, respectively.

2.2. Force field and simulations methods

We adopted an all-atom approach to model the linoleate (LIN) molecules, the Na^+ ions, and the water. The bonded and non-bonded parameters for the LIN and the Na^+ species are taken from the CHARMM27 force field for lipids [22,23] with the default *cis* torsions parameters for the double bonds of the molecules. The TIP3 water model [24] was used for the solvent, consistently with the CHARMM prescription. Two systems were built using two different protocols each containing 60 monomers of LIN in all *trans* conformation, 60 Na^+ and 9997 water molecules. In the first approach, we constructed a *preformed* micelle (called M60-P, hereafter) with the Packmol program [25]. This program creates an initial starting point for the MD, by packing the corresponding numbers of LIN molecules in the sphere with the last methyl groups near the headgroups at ~23 Å from the center (i.e. slightly larger than the total length of linoleate molecules in order to reduce the number of 'steric clashes' for the terminal groups of LIN molecules). Subsequent minimization (with a conjugated gradient (CG) algorithm with a cutoff of 10 Å and equilibration periods in vacuum with small time steps) was performed to remove possible inter- and intra-molecular overlaps. After this step, the micelle was inserted in a truncated octahedron box ($a = b = c = 75$ Å and $\alpha = \beta = \gamma = 109.472^\circ$) of water with periodic boundary conditions. This size of the box ensures a sufficient solvation of the headgroups (~166 H_2O per lipid) and a sufficient distance (~15 Å) between the micelle surface and the edge and the cell boundaries to avoid artefacts due to the periodic conditions [26]. The resulting conformation was equilibrated during 350 ps at 450 K with the lipids fixed to quickly equilibrate the water and the Na^+ ions. Next, the system was set to $T = 0$ K and LIN molecules were freed, whereas the system was slowly heated to 300 K during 300 ps as described in [27]. Then, the micelle was simulated in the NPT ensemble at $P = 0.1$ MPa and $T = 300$ K and the data were collected during 10 ns after discarding the first 100 ps.

For the simulations of the self-aggregated system (called M60-S), 60 LIN molecules and 60 Na^+ ions were randomly placed in the same truncated octahedron box used in the case of preformatted micelle and also containing the same number of water molecules, i.e. 9997. This system was minimized with 500 time steps with CG and heated at 1000 K in the NVE ensemble during 100 ps to quickly randomize the lipids, the ions and the solvent molecules. After these steps, the system was simulated in the same NPT conditions as that used for M60-P during 31 ns after discarded the first 300 ps. Atomic configurations were saved every 240 fs (M60-P) and 480 fs (M60-S) for subsequent analysis.

For all simulations and analysis, we used the ORAC MD code [28]. ORAC uses the extended system approach for simulate in the NPT ensemble [29–33]. To integrate the equations of motions, we used a r-RESPA integrator with a 12 fs time step [34] combined with a Smooth Particle Mesh Ewald (SPME) [35] to handle electrostatic interactions and constraints method [36]. For both systems, we used a convergence parameter $\alpha = 0.43$ Å^{-1} and fifth-order B-spline with a 64 grid point for the SPME charge interpolation in order to maintain for all systems a relative error on the electrostatic interaction (<0.1%).

3. Results and discussion

For both M60-P and M60-S, at $P = 0.1$ MPa and $T = 300$ K, we obtained an average volume near 326400 Å^3 for a density close to 1.01 g cm^{-3}. Accordingly, the concentration of LIN in the two boxes is near 0.3 M, which is much larger than the experimental value of c.m.c. (2 mM at pH 11.4). Thus to simulate the system near the c.m.c. value, the number of water molecules must be increased by a factor of nearly 150 which is too time consuming for all-atoms simulations, even with current supercomputers capabilities. Besides, increasing the simulation box size will also increases the time necessary to obtain a stable and complete micelle [16] due to the large space between each LIN monomer and the diffusion time of the monomers through the water box.

The main goal of this work is to examine the influence of construction protocol on the LIN micelle structure in order to validate our model of micelles for future research and not to extract predictions on the kinetics of the micellization process. Thus, as the system still evolves towards one sole micelle in spite of the high concentration of simulated LIN solution, we also tested the influence of LIN concentration by performing an additional simulation at the same thermodynamic conditions than the micellar system with a 60 LIN monomers arranged in bilayer (with 30 LIN monomers by leaflet). We found that the LIN bilayer relaxed quickly (i.e. in 800 ps) towards a micelle with structural characteristics very close to that described hereafter for the M60-S and M60-P micellar systems.

3.1. Aggregation process of LIN micelle

In Fig. 1, we show snapshots at different periods of the M60-S run illustrating the micellization process, while in Fig. 2, we present the plots of the number of clusters, $n_{cluster}$, with respect to the time. Because the system concentration is well above the c.m.c. and since LIN molecules are mainly hydrophobic, the micelle aggregation process is fast, i.e. quicker than 10 ns. It presents two stages with a fast and a slow timescales: $t < \sim 2.0$ ns and ~ 2.0 ns $< t < \sim 10.0$ ns of the run, respectively. At the beginning of the run ($t = 480$ fs), 60 LIN molecules randomly placed in the water box are starting to form small clusters during the 100 ps of the equilibration period. During the fast stage ($t < \sim 2.0$ ns), these clusters aggregate, fragment and aggregate with a Smoluchowski-type mechanism [37] as shown by the fast decrease and by the variation of the value of $n_{cluster}$ with time. A similar behavior was also found by other authors with different surfactants [16,17,38–40]. At $t = \sim 2.0$ ns, a micelle is formed with ~55–56 monomers of LIN molecules and we estimate that ~10 ns are needed to obtain a stable and compact micelle formed of with all the 60 lipids.

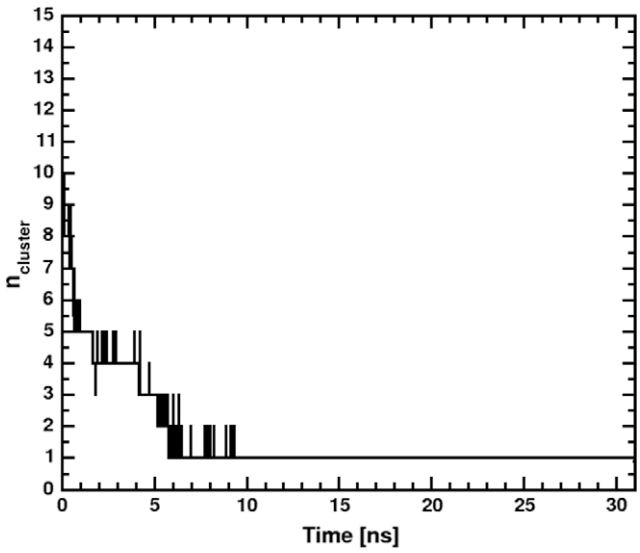

Fig. 2. Appearance and disappearance of the total number of LIN clusters $n_{cluster}$ with the time for the M60-S simulation.

3.2. Shapes and sizes of the 'self-aggregated' and 'preformatted' micelles

In current MD approaches, it is a common practice to simulate preformed micelles in order to save computational time. It is therefore interesting to compare the structures of 'self-aggregated' and

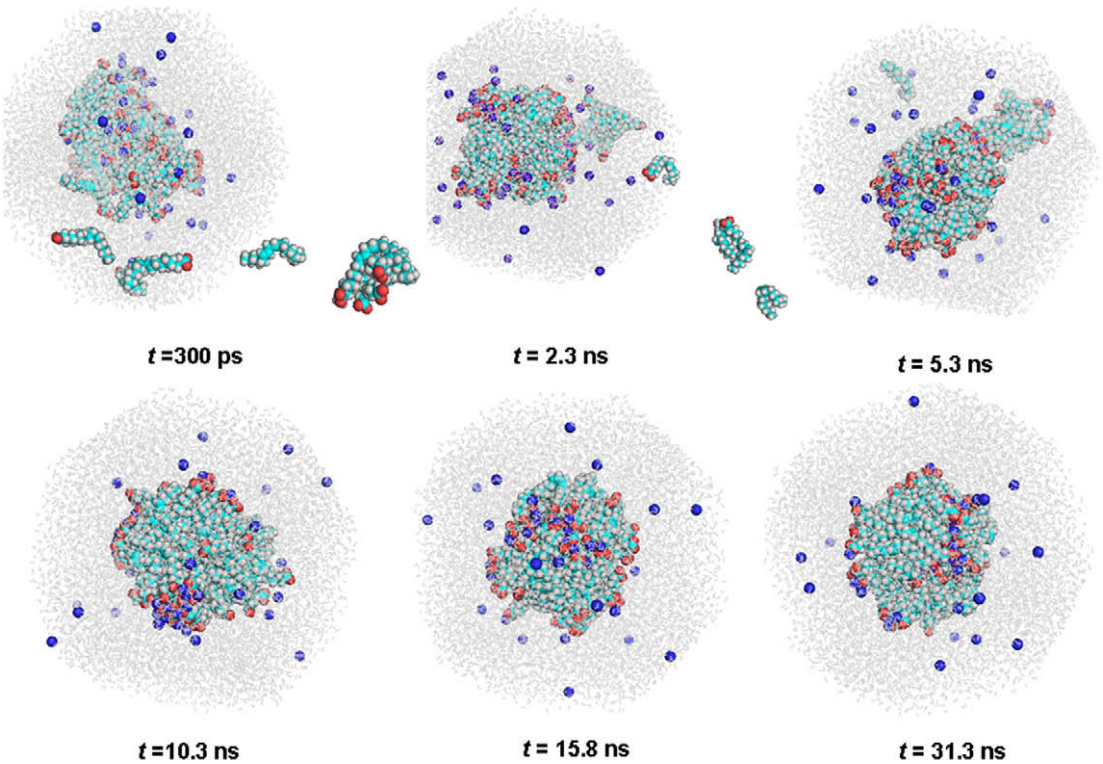

Fig. 1. Aggregation process of LIN monomers into a micelle vs. time. LIN and Na^+ molecules are drawn in CPK style while water is represented as gray lines. Note that the lipids outside the cells 1 and 2 are caused by the periodic bound conditions. Carbon, oxygen, hydrogen, and sodium ions are in magenta, red, white, and blue colors, respectively. Figures were drawn with PYMOL [49]. (For interpretation of the references to color in this figure legend, the reader is referred to the web version of this article.)

'preformatted' micelles, using the geometric model of LIN micelles with $N = 60$. For this purpose, we compared several properties of simulated micelles such as shape, dimension, lipid conformation, surface, and hydration properties. Analysis of the micellar shape was made by computing the average axial ratio a/c between the major and the minor semi-axis lengths obtained from the inertia tensors [27]. The average values of a/c are identical for the two kinds of micelles and equal to 1.23 ± 0.08 (value taken from 10 ns to 31 ns for M60-S and during all the run for M60-P). This indicates that, for both types of micelles, the final shape is not perfectly spherical and is independent of the method used to construct the self-assembly. It is difficult to compare these results with experimental studies since, to the best of our knowledge; there are no reports in literature at such a high micellar concentration. Nevertheless, as said in the introduction, several experimental studies were carried out with linoleate micelles in different environment (different concentrations, different counterions (K^+), and temperature) using SANS [12] and Cryo-TEM [3]. In this latter study, the authors showed that sodium linoleate micelles are mainly spherical. Note that the corresponding experimental resolution was not sufficient to estimate a possible eccentricity of the observed spheroids (Fig. 3). However, it should be emphasized that Johnson et al. in Ref. [12] have studied the structure of potassium linoleate microemulsions at a concentration close to 0.1 M and at 40 °C. To adjust their SANS scattering curves, the authors used the Hayter–Penfold model [41] and showed that the micelles display a prolate shape with an axial ratio of 1.18. This value obtained with a relatively large aggregation number ($N = 110$) remains clearly close to that we obtained using MD simulation.

For sodium linoleate micelles ($N = 60$), the Cryo-TEM cannot settle the argument between sphere and slightly ellipsoidal shape (Fig. 3). Indeed, the resolution on the apparent radius of spheroids in Cryo-TEM is not sufficient to estimate an eccentricity while in our case the SANS spectra can be fitted indifferently with prolate or spherical shape with comparable precision.

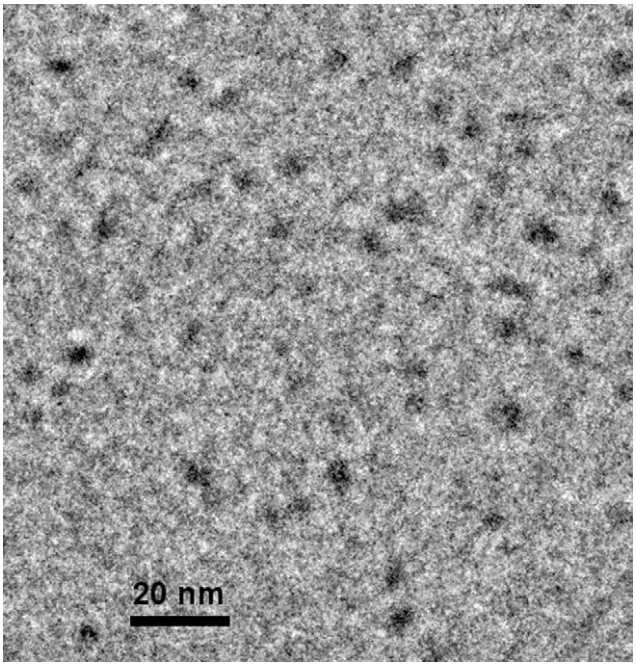

Fig. 3. Cryo-TEM image of solution containing 10 mM Lin-Na at pH 12.2 with micelles of average radius 20.0 ± 3.0 Å. The solution was deposited on a holey-carbon-coated grid and plunged into liquid ethane for quick freezing of the system. Observation was carried out at −180 °C in a JEOL 2100F electron microscope with a defocus about 2 μm and Contrast Transfer Function correction was applied on the resulting image.

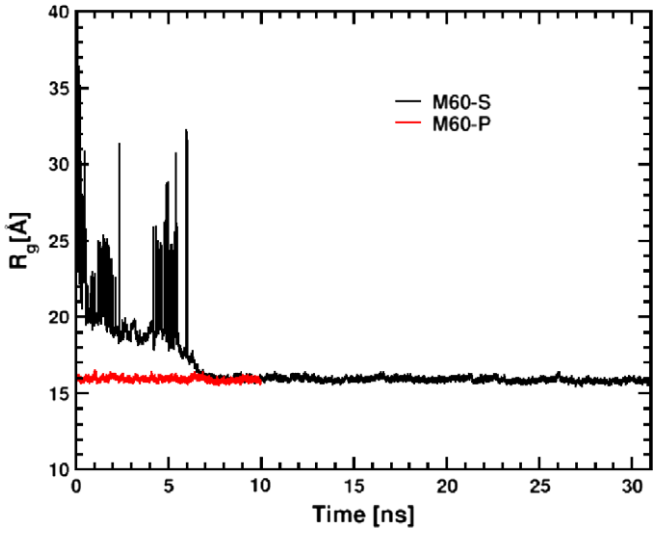

Fig. 4. Radius of gyration as a function of time for the two micelles studied.

In Fig. 4, we plotted the radius of gyration, R_g, as a function of time for both M60-P and M60-S micelles, computed with the following expression:

$$R_g^2 = \sum_i m_i (r_i - r_{cm})^2 / \sum_i m_i \quad (2)$$

where m_i is the mass of the atom i of the micelle at the distance r_i from the center of mass r_{cm} for all LIN monomers. As shown, the value of R_g for M60-S decreases during the self-aggregation process in the same manner as $n_{cluster}$ (Fig. 2). This is consistent with the fusion of LIN clusters into a large micelle. In the timeframe $t \approx 2$–10 ns, the R_g value of M60-S fluctuates around 18–32 Å due to 2 or 6 LIN monomers that remain free in the box (Fig. 1). After ~6 ns, R_g decreases and reaches a stable value of 16.0 ± 0.1 Å, as in the case of M60-P micelle, as shown in Fig. 3. From this R_g value, one gets the effective radius (R_M) values of the micelles modeled as a solid sphere of uniform density $R_M = \sqrt{5/3}R_g$ = 20.6 ± 0.1 Å [42,43]. This value is slightly larger than that estimated using the spherical model (19.5 Å) but remains consistent with the value obtained by Cryo-TEM for a sodium linoleate micelle (20.0 ± 3.0 Å) as shown in Fig. 3.

To compare the microenvironment of the two kinds of micelles as a function of the used protocol, we computed the average radial mass density profiles $\rho(r)$ with respect to the center of mass (COM) of the aggregate ($r = 0$ Å) [27]. Fig. 5 clearly indicates that the two types of micelles display similar microstructures and present an ionic layer extended for M60-P (~10.0 ± 0.5 Å). The oil core of both micelles extends from 0 to ~18 Å with an average density (~0.80 g cm^{-3}) close to the experimental density of a C17 alkyl chain (e.g. for the heptadecane ~0.78 g cm^{-3}) [44]. The $\rho(r)$ can also be used to estimate the micelle radius, R_M, with the average maximum of the density profile of the headgroup. The values for both micelles (R_M = 19.0 ± 0.5 Å) are in agreement with the previously calculated value assuming a spherical model (19.5 Å) and the micelle obtained by CRYO-TEM experiment.

3.3. Surface and hydration properties of the 'self-aggregated' and 'preformatted' micelles

In 2004, Bond et al. [39] examined the micellization process of 60 and 80 dodecylphosphocholine (DPC) monomers, by computing

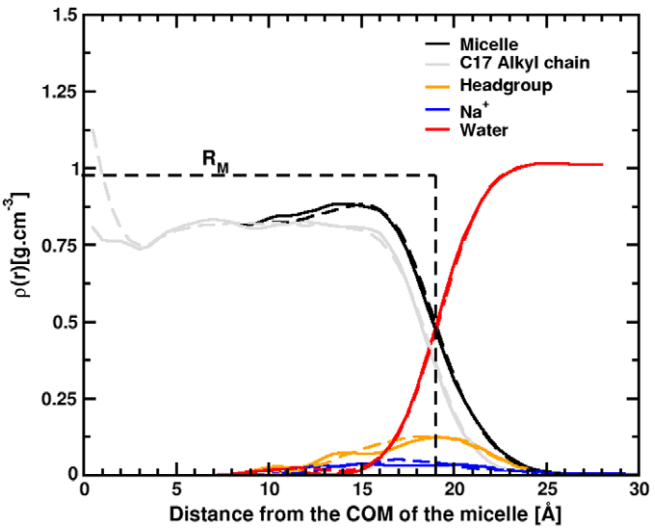

Fig. 5. Averaged radial profiles $\rho(r)$ with respect to the center of mass (COM) ($r = 0$ Å) for M60-S (dashed line) and M60-P (continue line) micelles. A 0.5 Å bin width was used. In the case of M60-S, the $\rho(r)$ was obtained from the last 21 ns of the run.

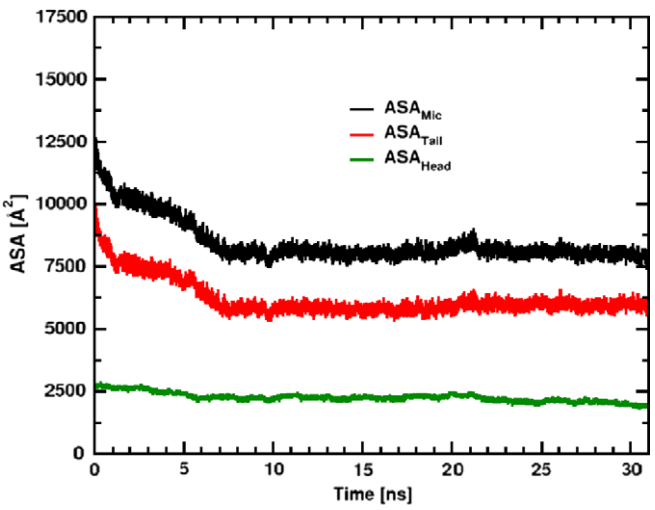

Fig. 6. Reduction of the accessible surface area (ASA) for the micelle (ASA_{Mic}), the hydrophilic head (ASA_{head}) and the C17 alkyl tail (ASA_{tail}) atoms computed with Voronoï polyhedral construction [45].

the variation of the total accessible surface area (ASA) of the micelle in contact with the water as a function of time. We used the same approach by computing the Voronoï surface [45,46] shared by water with the full micelle surface (ASA_{Mic}), the hydrophilic head surface (ASA_{head}) and the C17 alkyl tail surface (ASA_{tail}) (Fig. 6). The $ASA_{head,}$ which averages at 2168 ± 38 Å^2 remains nearly constant, in agreement with the fact that the headgroups of lipids are always fully accessible during all runs. The ASA_{Mic} and ASA_{tail} curves present fast and slow relaxations related, once again, to the collapse of LIN monomers into a micelle. Finally, for $t > 10$ ns, the values of ASA_{Mic} and ASA_{tail} converge to 8080 ± 173 Å^2 and 5894 ± 152 Å^2, respectively. These values are close to that of ASA_{Mic} and ASA_{tail} obtained for the preformed micelle (7912 ± 260 Å^2 and 5701 ± 145 Å^2). The hydrophilic surface fraction $f = (ASA_{head}/ASA_{Mic})$, is equal to 26.5% in the case of M60-S and is equal to 27.1% for M60-P. Those values are consistent with the geometric model predicting a hydrophilic surface fraction $f = 26.4\%$. Fig. 7 also shows that LIN headgroups form isolated patches of 5–6 (M60-P) and 2–3 (M60-S) headgroups at the micellar surface. The total surface area corresponding to these patches varies from 72 to 108 Å^2 and from 180 to 220 Å^2 in the case of M60-P and M60-S micelles, respectively. The existence of sodium (Na^+) saline bridges corresponding to the headgroups-water interactions, the deprotonation of LIN molecules and the resulting electrostatic interaction are more likely to counterbalance the entropy loss in the gathering of the headgroups and thus may favor the formation of the patches [47].

3.4. Lipid conformation

We computed the average end-to-end distance probability distribution $P(r)$ [27] between the two terminal carbon atoms present at the extremities of the alkyl chain, or d_{c18}. For (M60-P) and (M60-S), $P(r)$ displays peaks at 18.2 ± 0.1 Å and 17.6 ± 0.1 Å, respectively (data not shown). Due to the confinement and the hydrophobic repulsion induced by the two double bonds, the values we obtained for the C18 alkyl tail of linoleate molecule is significantly shorter than that which was previously calculated by Johnson et al. (21.8 Å) [12]. Further investigations show that in these micelles, linoleate molecules adopt, on average, a pseudo-cycloid arrangement (Fig. 8) caused by the *cis* configuration of the two double bonds [20]. Indeed, the dihedral angles involved in these bonds are slightly *cis* with a relative population $p_{cis} = 55.0\%$ and $p_{cis} = 58.0\%$ for M60-P and M60-S, respectively. The slight difference between the two relative populations can be due to the high temperature equilibration step for M60-S system, that has probably favored the double bonds dihedral transition from *trans* to *cis*.

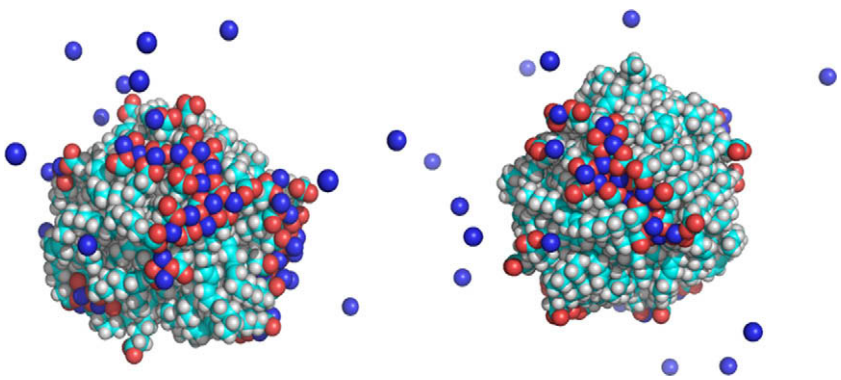

Fig. 7. Snapshots of the M60-P and M60-S LIN micelles at $t = 10$ ns (left) and $t = 31$ ns (right). Color coding is the same as the Fig. 1. Water molecules are removed for visual clarity. (For interpretation of the references to color in this figure legend, the reader is referred to the web version of this article.)

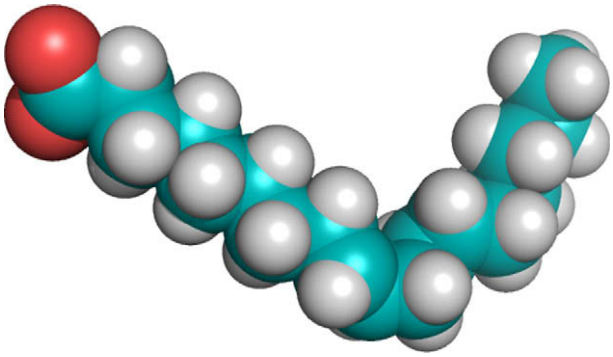

Fig. 8. Example of a linoleic acid molecule conformation taken from the M60-S simulation. Same color coding as in Fig. 1. (For interpretation of the references to color in this figure legend, the reader is referred to the web version of this article.)

3.5. Interfacial properties; ions and water distribution

To obtain more data concerning ions and water distribution around the micelle, we computed the number of Na^+ sodium ions and of water molecules interacting with the oxygen atoms of the carboxylate LIN headgroups. For this purpose, we used the radial density function, $g(r)$ and by integrating this function until the first minimum of the first peak at ~3.0 Å and at ~3.6 Å for Na^+–COO^- and H_2O–COO^- pairs, respectively, one can obtain the average number of nearest neighbors for each LIN headgroup oxygen atom. Our values indicate no difference between the two kinds of micelles. For Na^+–COO^- interaction, the number of Na^+ ions in its first shell is 0.9–1.2. Figs. 1 and 6 also show that Na^+ ions can interact favorably with 2 or 3 LIN headgroups and also located far from the micelle surface. For the hydration of oxygen atoms, the averages numbers of water molecules in its first shell are 3.5 (M60-S) and 3.9 (M60-P), in agreement with the values obtained by Jorgensen and Gao [48] in the case of carboxylate ions in water studied using Monte Carlo simulation (3.4 H_2O molecules/carboxylate oxygen).

4. Conclusion

In this Letter, we examined, by computer simulation, the influence of the construction protocol on the structure of linoleate micelles (C18:2) at a high lipid concentration (near 0.3 M) in water, at pH 7. The spontaneous aggregation of LIN monomers into a micelle is fast, less than 10 ns, and undergoes two stages: aggregation of single monomers into small clusters and then micelle formation by clusters coalescence. The micelle obtained at $t = 10$ ns is stable with a structure very similar to the one constructed with the preformed approach. The two kinds of micelles display similar dimensions (20 Å) and a slightly ellipsoidal shape with an average major-to-minor semi-axis ratio close to 1.2. The micellar surfaces are mainly hydrophobic, 73% of the surface being covered by LIN tails. Na^+ sodium ions are restricted to the micelle polar layer and interact with 2–3 LIN headgroups. These results are consistent with the geometric model used to construct the preformed micelle and with the dimension of LIN micelle deduced from Cryo-TEM observations. In conclusion, our results present a good model for the description of linoleate micelle in water and certainly offer a good starting point to study the structure of such a system in a more complex environment.

Acknowledgements

This work was granted access to the HPC resources of CCRT/CINES under the allocation 2009-t2009076076 made by GENCI (Grand Equipement National de Calcul Intensif).

References

[1] V. Pala et al., J. Natl. Cancer Inst. 93 (2001) 1088.
[2] K. Holmberg, B. Jönsson, B. Kronberg, B. Lindman, Surfactants and Polymers in Aqueous Solution, second edn., John Wiley & Sons, New York, 2002.
[3] J. Attia, S. Remita, S. Jonic, E. Lacaze, M.C. Faure, E. Larquet, M. Goldmann, Langmuir 23 (2007) 9523.
[4] F. Reiss-Husson, V. Luzzati, J. Phys. Chem. 68 (1964) 3504.
[5] J.N. Israelachvili, Intermolecular and Surface Forces, Academic Press, New York, 1992.
[6] R. Zana, Dynamics of Surfactant Self-Assemblies: Micelles, Microemulsions, Vesicles and Lyotropic Phases, CRC Press, 2005.
[7] J.M. Gebicki, M. Hicks, Chem. Phys. Lipids 16 (1976) 142.
[8] M.L. Rogerson, B.H. Robinson, S. Bucak, P. Walde, Colloids Surf. B 48 (2006) 24.
[9] J.M. Gebicki, A.O. Allen, Phys. Chem. 73 (1969) 2443.
[10] J.W. Mc Bain, W.C. Sierichs, J. Am. Oil Chem. Soc. 25 (1948) 221.
[11] J. Borne, T. Nylander, A. Khan, Langmuir 17 (2001) 7742.
[12] J.S. Johnson, W.L. Griffith, A.L. Compere, Langmuir 5 (1989) 1191.
[13] M.L. Klein, W. Shinoda, Science 321 (2008) 798.
[14] M. Tarek, S. Bandyopadhyay, M.L. Klein, J. Mol. Liq. 1–2 (1998) 1.
[15] J.-B. Maillet, V. Lachet, P.V. Coveney, Phys. Chem. Chem. Phys. 1 (1999) 5277.
[16] S.J. Marrink, D.P. Tieleman, A.E. Mark, J. Phys. Chem. B 104 (2000) 12165.
[17] M. Jorge, Langmuir 24 (2008) 5714.
[18] T.H. Haines, Proc. Natl. Acad. Sci. 80 (1983) 160.
[19] R. Klein, M. Kellermeier, M. Drechsler, D. Touraud, W. Kunz, Colloids Surf., A 338 (2009) 129.
[20] D.M. Small, The Physical Chemistry of Lipids, Plenum Press, New York, 1986.
[21] C. Tanford, J. Phys. Chem. 76 (1972) 3021.
[22] A.D. MacKerell, B. Brooks, I.C.L. Brooks, L. Nilsson, B. Roux, Y. Won, M. Karplus, CHARMM: The Energy Function and its Parameterization with an Overview of the Program, John Wiley & Sons, Chichester, 1998.
[23] S.E. Feller, K. Gawrisch, A.D. MacKerell, J. Am. Chem. Soc. 124 (2002) 318.
[24] W.L. Jorgensen, J. Chandrasekhar, J.D. Madura, R.W. Impey, M.L. Klein, J. Chem. Phys. 79 (1983) 926.
[25] J.M. Martínez, L. Martínez, J. Comp. Chem. 24 (2003) 819.
[26] P.H. Hunenberger, J.A. McCammon, Biophys. Chem. 78 (1999) 69.
[27] S. Abel, F. Sterpone, S. Bandyopadhyay, M. Marchi, J. Phys. Chem. B 108 (2004) 19458.
[28] P. Procacci, T.A. Darden, E. Paci, M. Marchi, J. Comp. Chem. 18 (1997) 1848.
[29] H.C. Andersen, J. Chem. Phys. 72 (1980) 2384.
[30] M. Parrinello, A. Rahman, J. Appl. Phys. 52 (1981) 7182.
[31] A. Rahman, F.H. Stillinger, J. Chem. Phys. 55 (1971) 3336.
[32] S. Nose, J. Chem. Phys. 81 (1984) 511.
[33] W.G. Hoover, Phys. Rev. A 31 (1985) 1695.
[34] M. Marchi, P. Procacci, J. Chem. Phys. 109 (1998) 5194.
[35] U. Essmann, L. Perera, M.L. Berkowitz, T. Darden, H. Lee, L.G. Pedersen, Chem. Phys. 103 (1995) 8577.
[36] J.P. Ryckaert, G. Ciccotti, H.J.C. Berendsen, J. Comp. Chem. 23 (1977) 327.
[37] S. Cueille, C. Sire, Europhys. Lett. 40 (1997) 239.
[38] J.-B. Maillet, V. Lachet, P.V. Coveney, Phys. Chem. Chem. Phys. 1 (1999) 5277.
[39] P.J. Bond, J.M. Cuthbertson, S.S. Deol, M.S.P. Sansom, J. Am. Chem. Soc. 126 (2004) 15948.
[40] X. Jun, S. Wenqi, L. Ganzuo, Z. Gaoyong, Chem. Phys. Lett. 438 (2007) 326.
[41] J.B. Hayter, J. Penfold, J. Chem. Soc., Faraday Trans. 77 (1981) 1851.
[42] C.D. Bruce, M.L. Berkowitz, L. Perera, M.D.E. Forbes, J. Phys. Chem. B 106 (2002) 3788.
[43] S. Bogusz, R.M. Venable, R.W. Pastor, J. Phys. Chem. B 104 (2000) 5462.
[44] B.D. Smith, R. Srivastava, Thermodynamic Data for Pure Compounds, Elsevier, New York, 1986.
[45] G.F. Voronoi, J. Reine Angew. Math. 134 (1908) 198.
[46] P. Procacci, R. Scateni, Int. J. Quantum Chem. 42 (1992) 1515.
[47] E. Ruckenstein, J.A. Beunen, Langmuir 4 (1988) 77.
[48] W.L. Jorgensen, J. Gao, J. Phys. Chem. 90 (1986) 2174.
[49] W.L. DeLano, The Pymol Molecular Graphics System. DeLano Scientific, San Carlos, CA., 2002.